Please cite this article in press as: Söding et al., Mechanisms for Active Regulation of Biomolecular Condensates, Trends in Cell Biology (2019), https://doi.org/10.1016/j.tcb.2019.10.006

CellPress REVIEWS

Opinion

Mechanisms for Active Regulation of Biomolecular Condensates

Johannes Söding,[1,*] David Zwicker,[2] Salma Sohrabi-Jahromi,[1] Marc Boehning,[3] and Jan Kirschbaum[2]

Liquid–liquid phase separation is a key organizational principle in eukaryotic cells, on par with intracellular membranes. It allows cells to concentrate specific proteins into condensates, increasing reaction rates and achieving switch-like regulation. We propose two active mechanisms that can explain how cells regulate condensate formation and size. In both, the cell regulates the activity of an enzyme, often a kinase, that adds post-translational modifications to condensate proteins. In enrichment inhibition, the enzyme enriches in the condensate and weakens interactions, as seen in stress granules (SGs), Cajal bodies, and P granules. In localization-induction, condensates form around immobilized enzymes that strengthen interactions, as observed in DNA repair, transmembrane signaling, and microtubule assembly. These models can guide studies into the many emerging roles of biomolecular condensates.

Biomolecular Condensates Can Be Formed and Dissolved in the Blink of an Enzyme

Eukaryotic cells possess numerous types of **membraneless organelles** (see Glossary). Each contains between tens and several thousands of protein and RNA species that are highly enriched compared with the surrounding nucleoplasm or cytoplasm. These biomolecular **condensates** are held together by weak, multivalent, and highly collaborative interactions, often between intrinsically disordered regions of their constituent proteins [1,2].

In contrast to membrane-bound organelles, biomolecular condensates can easily be formed or dissolved by merely changing the activity of an enzyme, such as a kinase, that post-translationally modifies key condensate proteins [3–5,71]. The modifications usually lie in intrinsically disordered regions and modulate the strength of attractive interactions with other condensate components [6,7]. Due to the highly cooperative nature of **phase transitions**, small changes in interaction strengths can result in the formation or dissolution of condensates, and this switch-like nature makes them ideal for dynamic regulation.

For instance, SGs form on cellular stress and are dissolved when the stress ceases [3]. Also, P-bodies in the cytoplasm and Cajal bodies, nuclear speckles, paraspeckles, and PML bodies in the nucleus have to be dissolved during mitosis and reformed afterwards to ensure a balanced distribution of their contents to daughter cells [4,8].

These droplet organelles are large enough to be visible using simple light microscopy techniques and have long been known. Recently, **liquid–liquid phase separation** has been implicated in multifarious processes in which – often submicrometer-sized – condensates are formed at particular locations in the cell: at sites of DNA repair [9], Polycomb-mediated chromatin silencing [10], transmembrane signaling [11,12], microtubule formation [13–15], actin polymerization [16], endocytosis [17,18], presynaptic active zones [19,20], and ribonucleoprotein (RNP) transport [21–23]. Such localized condensates form on a local stimulus to recruit the required set of proteins and are dissolved once their job is done.

Cells do not only need to regulate the formation and dissolution of each type of condensate. They sometimes also need to regulate their size and with it their numbers, to allow many condensates to form in different locations; for instance, to activate many genes at the same time [24–27]. Here, we propose two active mechanisms used by cells for these purposes.

Highlights

Biomolecular condensates are phase-separated domains in the nucleoplasm or cytoplasm formed by weak and highly multivalent interactions between their protein and RNA components. They allow cells to create compartments strongly enriched or depleted in specific proteins or RNAs, without the need for membranes.

Cells can actively regulate the formation, dissolution, and localization of condensates by phosphorylation and other post-translational modifications of condensate components.

We propose two unifying, generic mechanisms of active regulation. In the first, the protein concentration is above saturation and the modifications limit the condensate size by inhibiting intracondensate interactions. We believe this mechanism regulates most membraneless organelles.

In the second mechanism, the protein concentration is below saturation, but localized enzymes attach modifications that promote interactions and induce condensate formation in the volume around them. This mechanism can explain how a single kinase (e.g., recruited to a double-strand DNA break) can recruit hundreds of specific proteins.

We argue that many types of condensates are actively regulated by one of these two mechanisms.

[1]Quantitative Biology and Bioinformatics, Max Planck Institute for Biophysical Chemistry, Am Fassberg 11, 37077 Göttingen, Germany

[2]Max Planck Institute for Dynamics and Self-Organization, Am Fassberg 17, 37077 Göttingen, Germany

Please cite this article in press as: Söding et al., Mechanisms for Active Regulation of Biomolecular Condensates, Trends in Cell Biology (2019), https://doi.org/10.1016/j.tcb.2019.10.006

Phase Separation and Condensate Size Behavior

To keep the models simple, we consider only one type of condensate protein. In the dilute regime below the saturation protein concentration c_{out}, no condensate can form (Figure 1A). Above c_{out}, in the phase separation regime, condensates can be stable.

However, in a passive system more than one condensate cannot exist in equilibrium because larger condensates will grow at the expense of smaller ones (Figure 1B). The reason is that proteins on the surface of small droplets have fewer favorable interactions among themselves than proteins on the surface of larger droplets, due to the difference in surface curvature. They are therefore more easily lost, resulting in a higher equilibrium concentration outside the droplet (section 1.1 in the supplemental information online). Due to this size dependence, the protein concentration decreases from small to large condensates, and the decrease generates a diffusive flux in the direction of steepest descent. Consequently, there exists a critical radius R_{crit} below which condensates will shrink, while condensates above R_{crit} will grow (Figure 1C and section 1.2 in the supplemental information online). The critical radius increases until a single large condensate survives, a phenomenon called coarsening [28].

The timescale for droplets to change their size by coarsening scales roughly with their radius cubed (derived in section 1.3 in the supplemental information online). Therefore, small droplets can grow or shrink fast, on a scale of minutes for $R \approx 100$ nm, whereas droplets of a micrometer radius already take days. This explains why, in *in vitro* experiments, droplets of micrometer size and above can coexist for long periods.

We now show that, to actively regulate the formation and size of liquid droplet condensates, two generic mechanisms exist. A protein concentration maintained above saturation leads to the enrichment-inhibition model, in which a regulating enzyme such as a protein kinase inhibits favorable interactions and is enriched in condensates. A concentration maintained below saturation leads to the localization-induction model, in which the enzyme is localized or attached and induces favorable interactions. Although simplified, these models might capture two essential mechanisms for active regulation of cellular condensates.

Both mechanisms modulate interaction strengths of key condensate proteins by an enzyme that adds or removes post-translational modifications. Often, the regulating enzyme will be a kinase that attaches phosphoryl groups to disordered regions of condensate proteins. However, other post-translational modifications could take this role: poly-ADP-ribosylation in DNA repair [9], SUMOylation (e.g., in PML bodies [29]), arginine demethylation of proteins in RNA granules [30,31], lysine acetylation and methylation [15,32], ubiquitination [33], and RNA modifications [34,35]. Even RNA helicase activity can take over this role in RNA-containing condensates [36].

The Enrichment–Inhibition Model

Above the saturation concentration, a mechanism must exist that limits the size of larger condensates to allow the coexistence of multiple condensates. This can be achieved if the loss of proteins from the condensate increases faster with condensate radius R than the gain by net diffusive influx. The influx is proportional to $R - R_{crit}$ (Figure 1C). A loss that scales with the condensate volume $(4\pi/3)R^3$ would grow faster than $R - R_{crit}$. Above a certain radius, the loss would surpass the influx, shrinking condensates that are too large and thereby resulting in a stable condensate size.

We propose the loss mechanism to be the modification of condensate proteins (or RNA) by an antagonistic regulating enzyme (orange) that is itself enriched in the condensate (Figure 2, Key Figure). We use phosphorylation as an example, but the mechanisms work the same for other modifications. Because the concentration of unphosphorylated proteins (blue) is approximately constant in the condensate, the phosphorylation rate scales with the condensate volume. In this model, unphosphorylated proteins as well as the kinases attract each other, while the phosphorylation weakens the interactions with other condensate proteins. It might seem counterintuitive that the droplet-dissolving kinase enriches in the droplet, yet it is this feature that allows the droplet growth to be self-limiting.

[3]Department of Molecular Biology, Max Planck Institute for Biophysical Chemistry, Am Fassberg 11, 37077 Göttingen, Germany

*Correspondence: soeding@mpibpc.mpg.de

Please cite this article in press as: Söding et al., Mechanisms for Active Regulation of Biomolecular Condensates, Trends in Cell Biology (2019), https://doi.org/10.1016/j.tcb.2019.10.006

Since the concentration of the unphosphorylated proteins is above saturation, the concentration decreases towards the condensate, leading to a net influx of unphosphorylated proteins (Figure 2A). This influx is compensated by the loss of proteins that become phosphorylated inside the condensate, which diffuse out along the negative concentration gradient. Outside, they are dephosphorylated by phosphatases (green), closing the circle of protein flux.

To avoid wasting energy by a short-circuited phosphorylation–dephosphorylation reaction, the phosphatase and kinase would best be concentrated in different phases. Therefore, we expect the phosphatase to be strongly depleted in the condensates.

For phosphorylation rates k below a certain threshold k_{thr}, all condensates will grow or shrink to the same stable radius R, which is determined by k (Figure 2B and section 2 in the supplemental information online). The dependence of R on the phosphorylation rate k has a switch-like behavior (Figure 2C): above k_{thr}, no condensates can exist.

Evidence Supporting Enrichment-Inhibition

We give five examples of biomolecular condensates that behave as expected from the enrichment-inhibition model: (i) their key condensate proteins are phosphorylated by a kinase, (ii) increased kinase activity dissolves the condensates, and (iii) the kinase is enriched in the condensates. The model also predicts the main phosphatase to be depleted in the condensates. This information appears to be mostly unavailable.

'P granules' are condensates of RNAs and proteins in the one-cell embryo of the worm *Caenorhabditis elegans*. These localize to the posterior end of the cell and after cell division end up in the one cell that will give rise to the germ line. P granules are highly enriched for the intrinsically disordered MEG proteins. (i) They are phosphorylated by MBK-2 and dephosphorylated by the PPTR-1 phosphatase. (ii) Phosphorylation of MEGs promotes granule disassembly and dephosphorylation promotes assembly. Furthermore, (iii) MBK-2 localizes to P granules [37].

The vertebrate ortholog of MBK-2, DYRK3, plays a central role as dissolvase of several types of membraneless organelles during mitosis. Rai *et al.* suggested that, as for P granules, DYRK3 is involved in the size control of many other types of condensates [4], as we would expect from the enrichment-inhibition model.

'SGs' are another example. (i) They are regulated by DYRK3 [3]. However, since DYRK family kinases are constitutively active, it is unclear how the stress signal could be quickly relayed via DYRK3. Wurtz and Lee proposed a plausible mechanism [38]: on stress, ATP levels can fall by 50%, within the same timescale as SG formation. Also, ATP depletion alone is sufficient to induce SG formation. The reduction in DYRK3 activity (k in Figure 2C) by ATP depletion might reduce the level of phosphorylation of its targets, (i) several of which are key SG proteins. (ii) The concomitant increase in favorable interactions then would trigger SG formation. (iii) In accord with the enrichment-inhibition model, DYRK3 localizes to SGs [3].

'Nuclear speckles' concentrate proteins involved in pre-mRNA splicing. These factors possess a terminal low-complexity RS region enriched for arginine and serine, which is required for the multivalent interactions within the speckles [39]. (i) The CLK kinase phosphorylates the RS domains of splicing factors and (ii) phosphorylation by CLK promotes the disassembly of nuclear speckles [40]. Finally, (iii) CLK itself possesses an RS domain that is required and sufficient for its enrichment in the speckles [41].

'Cajal bodies' are nuclear condensates defined by the key architectural self-oligomerizing protein coilin. (i,ii) Hyperphosphorylation of coilin by Cdk2/cyclin E dissolves them. Also, (iii) Cdk2/cyclin is strongly enriched in Cajal bodies [42].

'Synaptic vesicles (SVs)' containing neurotransmitters form dense clusters at synapses. Synapsin, the major constituent of the matrix around SVs, forms condensates under physiological conditions *in vitro* [43]. The condensates enrich small lipid vesicles, explaining SV clustering at synapses. As expected, (i)

Glossary

Condensate: the protein-rich liquid, gel-like, or solid phase in the liquid cytoplasm or nucleoplasm. Liquid condensates are usually spherical to minimize the energetically unfavorable interface with the dilute phase. However, their shape can be influenced by scaffolding structures as in the case of chromatin. Their content is exchanged rapidly with the surroundings by diffusion. The mean retention time can be on the order of seconds or below, even for proteins highly enriched in the condensate.
Liquid–liquid phase separation: in mixtures of two or more components (e.g., proteins and water molecules), it may be energetically favorable for the components to separate into two liquid phases of different relative concentrations. For example, if proteins attract each other but have less favorable interactions with water, they can condense into liquid droplets with high protein concentration in a dilute phase of low protein concentration.
Membraneless organelles: biomolecular condensates that organize cytoplasmic and nucleoplasmic space, such as nucleoli, nuclear speckles, PML bodies, Cajal bodies, paraspeckles, SGs, and P-bodies.
Phase transition: transitions between states of matter determined by their interactions. Examples are the transition of a gas to a liquid state (condensation) or from a solid to a liquid state (melting). When two phases coexist (e.g., ice in water, water droplets in water vapor), we speak of phase separation.

Please cite this article in press as: Söding et al., Mechanisms for Active Regulation of Biomolecular Condensates, Trends in Cell Biology (2019), https://doi.org/10.1016/j.tcb.2019.10.006

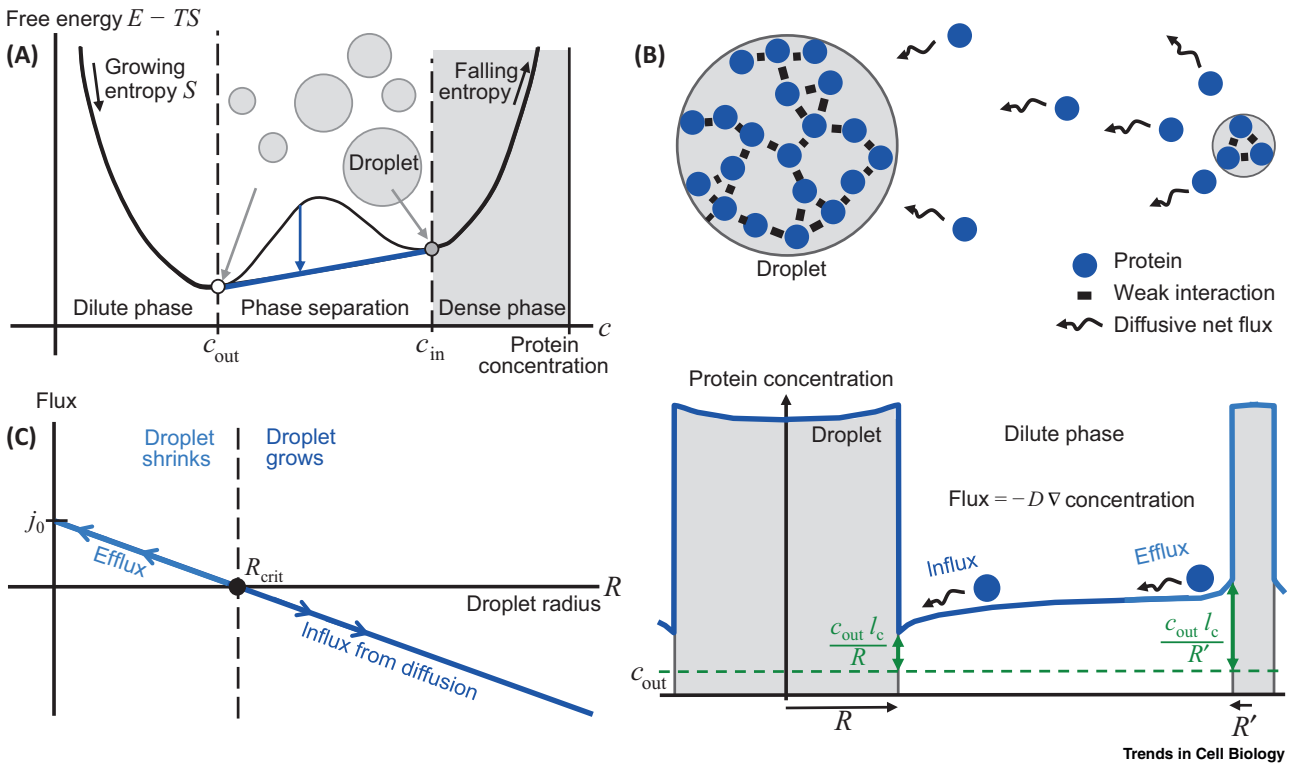

Figure 1. Phase Separation and Condensate Droplet Size Behavior.
(A) When protein–protein and solvent–solvent interactions are more favorable than protein–solvent interactions, demixing into two phases can occur: a dilute phase with low protein concentration c_{out} and a dense phase with high concentration c_{in}. This happens when the sum of the free energies of the two phases is lower (tip of blue arrow) than the energy of the single phase (base of arrow). T, temperature. (B) c_{out} is the limiting concentration for infinite condensate droplet radius. The concentration just outside a condensate increases with decreasing droplet radius (green double-headed arrows), as small droplets cannot hold on to their proteins as well as large ones. This creates a concentration gradient (r), which fuels a diffusive flux from small to large droplets (wiggly arrows). D, diffusion coefficient; l_c, protein–protein interaction strength. (C) As a result, condensates below a radius R_{crit} will shrink and larger ones will grow.

CaMKII kinase phosphorylates synapsin, (ii) its activity dissolves SV clusters *in vivo* in the presence of ATP, and (iii) CaMKII localizes to the condensates [43].

The Localization-Induction Model

Below the saturation concentration, no condensates can form. However, it is possible to locally push the concentration of proteins above saturation. This could be achieved if, in contrast to the previous model, the modifying enzyme acts agonistically and the modified proteins are attracted to each other through multivalent interactions, while the unmodified proteins have little or no affinity for each other and other condensate proteins. With that assumption, the locally confined addition of modifications represents a source of condensate proteins. This replenishment can compensate the diffusive loss that, below saturation, would otherwise cause the fast shrinkage and disappearance of any condensate.

Figure 3A illustrates the model with the example of phosphorylation. Proteins are phosphorylated at the site where the kinases are attached or bound, near the center of the condensate. From there, phosphorylated proteins diffuse out along the negative gradient of the concentration, which drops towards the outside. Outside the condensate, the phosphorylated proteins are dephosphorylated by phosphatases. The dephosphorylated proteins diffuse in towards the center of the condensate to the point of lowest concentration, where the kinase activity depletes them, closing the circle of protein flux.

Please cite this article in press as: Söding et al., Mechanisms for Active Regulation of Biomolecular Condensates, Trends in Cell Biology (2019), https://doi.org/10.1016/j.tcb.2019.10.006

Key Figure

Enrichment-Inhibition Model

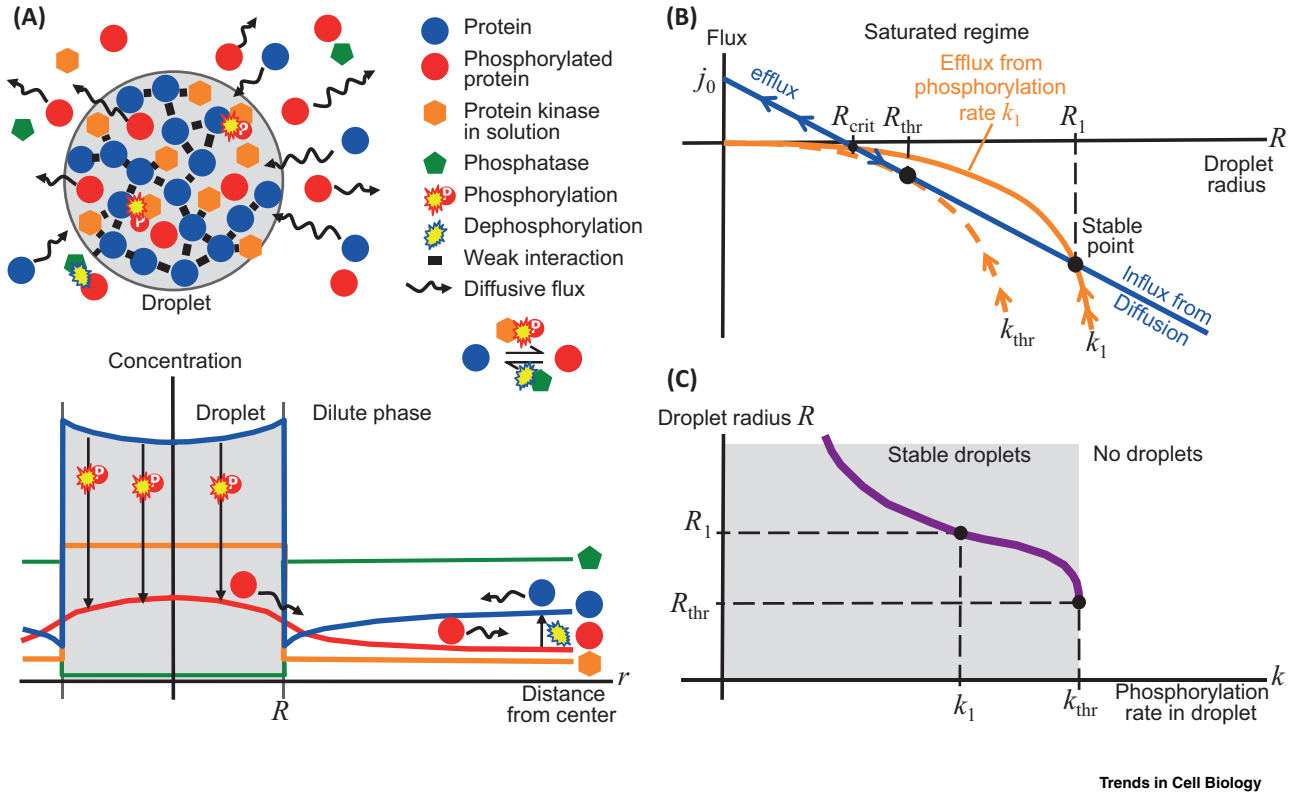

Figure 2. Condensate droplets can form when the concentration of unphosphorylated proteins is above the saturation concentration c_{out}. Phosphorylation weakens protein interactions, so condensates can be dissolved by increasing kinase activity. (A) The unphosphorylated proteins (blue) and kinase (orange) become concentrated in the condensates via multivalent, attractive interactions. There, the kinase phosphorylates condensate proteins (red bursts). The noninteracting phosphorylated proteins (red) diffuse out of the condensate. Outside, they are dephosphorylated (blue burst). Unphosphorylated proteins diffuse back into the condensate along the gradient of concentration (blue), compensating the outward flux of phosphorylated proteins. (B) Without losses from phosphorylation, condensates in the phase separation regime grow by diffusive influx if their radius R is above a critical value R_{crit}, whereas small condensates shrink (blue arrows). Because the influx grows linearly with condensate radius R whereas loss through phosphorylation grows with the condensate volume $(4\pi/3)R^3$ (orange), a stable radius R_1 results. (C) This radius depends on the phosphorylation rate k and shows a switch-like response.

For phosphorylation rates Q below a certain threshold Q_{thr}, no condensates can form (Figure 3B) because the efflux from a tiny drop is larger than the rate with which the kinases generate phosphorylated proteins. Above Q_{thr}, the condensate radius R depends linearly on kinase activity (Figure 3C and section 3 in the supplemental information online). As before, we expect the phosphatase to be depleted in the condensates.

In summary, the model provides a possible explanation for how condensates can be created and dissolved at specific cellular locations by regulating the activity of enzymes that add post-translational modifications to condensate components that enhance their interactions with other components.

Analogous to three dimensions, phase separation can occur in two dimensions above a certain saturation surface density, with the formation of clusters of high density surrounded by low-density regions [11,12].

Please cite this article in press as: Söding et al., Mechanisms for Active Regulation of Biomolecular Condensates, Trends in Cell Biology (2019), https://doi.org/10.1016/j.tcb.2019.10.006

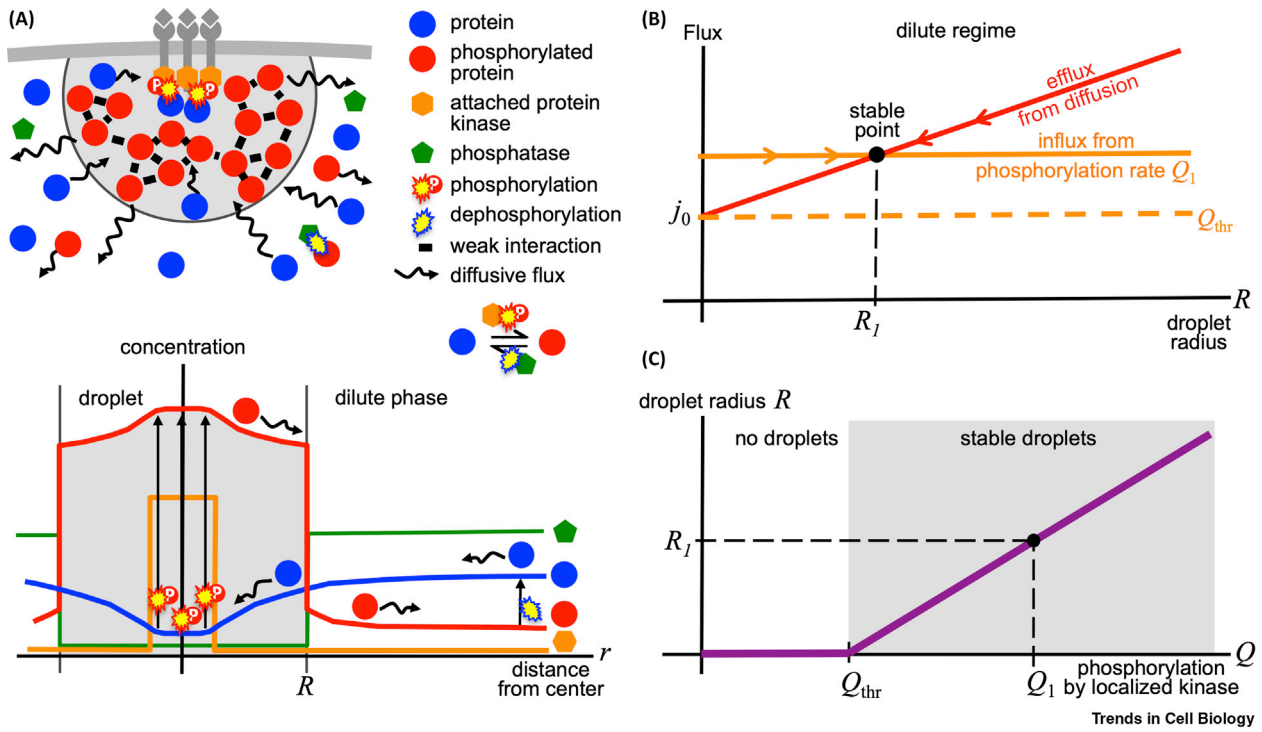

Figure 3. Localization-Induction Model.

(A) Condensates can form when kinases (orange), bound or attached to a cellular structure such as a membrane, locally phosphorylate proteins (blue). This raises the local concentration of the phosphorylated proteins (red), which bind to each other through multivalent interactions, above the threshold for phase separation. Because the concentration of phosphorylated proteins outside the condensate is below saturation, the condensate loses phosphorylated proteins through diffusive flux (wiggly arrows). Outside, they are dephosphorylated (blue burst). Unphosphorylated proteins diffuse back into the condensate, compensating the outward flux of phosphorylated proteins. (B) Without kinase activity (orange), condensates in the dilute regime would shrink rapidly by diffusive efflux. Because the kinase activity supplies phosphorylated proteins at a constant rate Q_1, a stable equilibrium is reached at radius R_1. Below rate Q_{thr}, no condensates can form. (C) Above Q_{thr}, stable condensates form, whose radius depends linearly on Q.

However, analogous to the 3D case, large clusters would grow at the expense of small ones in an unregulated fashion. A 2D extension of the localization-induction model could explain transmembrane receptor clustering upon binding to extracellular ligands and why some types of receptors organize into clusters of fixed size [12,44–46] (section 4 in the supplemental information online).

Evidence Supporting Localization-Induction

The localization-induction model makes three predictions. (i) The key regulating enzyme (e.g. a kinase) is targeted or attached to a specific cellular location, (ii) where it post-translationally modifies key condensate proteins. (iii) The modifications promote attractive interactions, leading to condensate formation around the site of the enzyme. Here we discuss examples of processes that behave as expected if they were regulated by the localization-induction model.

Upon the 'formation of a DNA double-strand break', (i) a poly(ADP-ribose) (PAR) polymerase-1 (PARP-1) protein will bind to the DNA break site, which allosterically triggers its autoactivation [47]. (ii) PARP-1 starts adding PAR to itself and target proteins. (iii) These recruit proteins with positively charged RGG-rich disordered regions, particularly FET proteins such as Fused in Sarcoma (FUS), via multivalent interactions with the negatively charged ADP-ribose subunits. Within seconds, a liquid condensate forms, which enriches the first-response factors at the damage site [9]. As expected, knockdown of the PAR-degrading enzyme PARG enhances the formation of DNA repair foci [48].

Please cite this article in press as: Söding et al., Mechanisms for Active Regulation of Biomolecular Condensates, Trends in Cell Biology (2019), https://doi.org/10.1016/j.tcb.2019.10.006

'T cell signal transduction' exemplifies localization induction in two dimensions. The T cell receptor kinase is phosphorylated and can then recruit and bind the membrane-bound ZAP70 kinase, which thereby becomes localized (i). The phosphorylation of T cell receptors also turns on the activity of its kinase domain, which phosphorylates and thereby activates the bound ZAP70 kinase. (ii) Activated ZAP70 phosphorylates the key membrane-bound protein LAT. (iii) Phosphorylation enables favorable interactions with several other proteins, with which LAT then forms a quasi-2D condensate at the inner plasma membrane surface. The condensate excludes the LAT-dephosphorylating phosphatase CD45 but recruits the machinery for actin assembly, which can form condensates of its own to induce cytoskeletal changes [49].

Many transmembrane signaling processes start by the formation of transmembrane receptor clusters. Case and colleagues [12] argue that many other transmembrane signaling processes (using glycosylated receptors, immune receptors, cell adhesion receptors, Wnt receptors, and receptor tyrosine kinases) possess features that suggest they too involve liquid–liquid phase separation.

The 'assembly of microtubules' is a further example. Metaphase centrosomes comprise a core structure called the centriole pair, surrounded by a condensed phase, the pericentriolar matrix [50]. (i) Condensate formation depends on the kinase PLK-1, which is concentrated at the centrioles and (ii) phosphorylates the key protein Cnn. Phosphorylated Cnn phase separates in *Drosophila* and enhances the nucleation of microtubules during mitosis. In accord with localization-induction (Figure 3C), the phosphorylation rate determines centrosome size [50], and Cnn proteins are continuously added to the condensate at the centrioles, where PLK-1 is bound [51].

Other Mechanisms of Size Control

Besides the two presented active mechanisms, a slower but fundamental way to regulate the formation of condensates is via transcriptional or translational control of the concentration of key components. For instance the formation and size of enhancer condensates [24,26,52,53] depends critically on the concentration of the transcription factors binding the enhancer.

In Figure 4, we propose the scaffolded condensate model, a passive mechanism that can keep condensates at a fixed size. For instance, the size of condensates formed at active enhancers might simply be confined by the space probed by the disordered regions of the transcription factors bound at the enhancer. The model might also explain the size control of paraspeckles and other nuclear condensates that assemble around long intergenic noncoding RNAs (lincRNAs) to recruit or sequester specific proteins [54]. Their lincRNAs act as a scaffold around which a condensate can form and their formation and size could be controlled via regulation of the lincRNA concentration.

In centrosomes of *C. elegans*, size is limited by the exhaustion of centrosome material [55,56]. Similarly, exhaustion of material might explain the size control of condensates formed around cytosolic dsDNA to launch an antiviral immune response [57]. Protein aggregation appears to be regulated by an active de-aggregation mechanism that kicks in only at large aggregate sizes, much above the critical radius [58]. Finally, condensates can be limited in size by mechanically preventing their coalescence [59].

The Models Make Testable Predictions

The presented models supply unifying principles to the often seemingly incoherent behavior of various types of biomolecular condensates. The enrichment-inhibition model predicts freely floating condensates in the cytoplasm or nucleoplasm to be size regulated by an antagonistic post-translationally modifying enzyme (e.g., a kinase) enriched in the condensates. The localization-induction model predicts spatially and temporally localized condensates such as those formed at sites of DNA repair to be regulated by an agonistic modifying enzyme at their center.

Please cite this article in press as: Söding et al., Mechanisms for Active Regulation of Biomolecular Condensates, Trends in Cell Biology (2019), https://doi.org/10.1016/j.tcb.2019.10.006

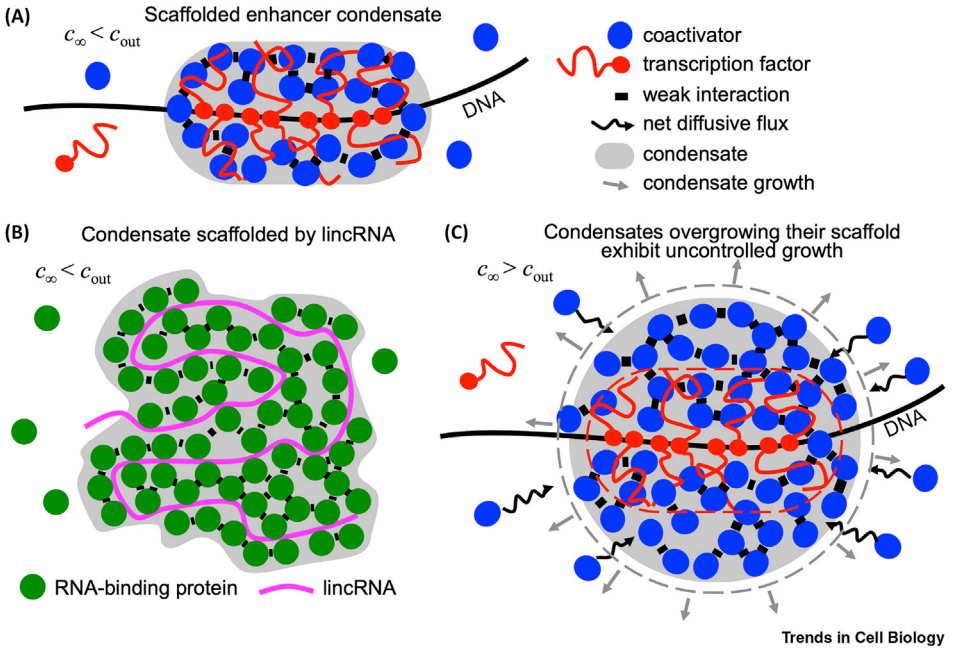

Figure 4. Scaffolded Condensate Model for Passive Size Control.
Without active mechanisms, when the concentration of proteins [blue in (A,C), green in (B)] is below saturation ($c_\infty < c_{out}$) condensates cannot form without help. However, their interaction with a localized scaffold [red in (A,C), pink in (B)] creates an attractive mean field potential $U(x)$ that, by Boltzmann's law, increases the local concentration at position x to $c_\infty e^{-U(x)kBT}$. If it surpasses c_{out}, a condensate forms whose spatial extent is confined by the mean field. (A) The disordered regions of transcription factors bound at an enhancer could interact with coactivators and thereby create an attractive mean field in which the coactivators can condense. (B) Analogously, long intergenic noncoding RNAs (lincRNAs) might be able to create an attractive mean field for RNA-binding proteins to condense in. (C) Below saturation, a passively regulated condensate cannot grow beyond its scaffold, because the protein fluxes through a condensate surface that has grown beyond the scaffold are independent of the scaffold and can therefore be stable only above saturation. Above saturation, the condensate location and size cannot be controlled.

To quantitatively test the enrichment-inhibition model *in vivo*, one could artificially induce the formation of membraneless organelles by partially inhibiting the antagonistic kinase enriched in them with a small-molecule inhibitor. The size of the condensates could be measured as a function of kinase activity and compared with the predictions from our theory (Figure 2C).

To quantitatively test the localization-induction model *in vivo*, one could apply corelet technology [69] to optically trigger the formation of 24-mer oligomers of the kinase suspected to induce the formation of condensates. The activity of the corelet-bound kinases can be modulated either by a small-molecular inhibitor or by expressing an inactive kinase from a controllable promoter. The resulting size of condensates can be compared with the model predictions (Figure 3C).

The localization-induction and the scaffolding models predict condensates to be stable even at very small radii (Figures 3C and 4A), at which the characteristic properties of phase separation are hard to observe by microscopy [70]. It is attractive to speculate that many previously detected protein clusters or foci might actually be tiny phase-separated liquid droplet condensates stabilized by the mechanisms in Figures 3 and 4. Recent molecular dynamics simulations of enhancers and experimental results indicate, for example, that the transcriptional minihubs observed in [24,26] might be true condensates [52]. Whether to call these clusters (e.g., the scaffolded condensates in Figure 4) bona fide condensates or not, their functional relevance might lie in their ability to achieve switch-like regulation through strong cooperatively.

Please cite this article in press as: Söding et al., Mechanisms for Active Regulation of Biomolecular Condensates, Trends in Cell Biology (2019), https://doi.org/10.1016/j.tcb.2019.10.006

Concluding Remarks

Zwicker *et al.* [60] and Wurtz and Lee [61] described how biochemically driven processes can be utilized for active size regulation of condensates. The enrichment-inhibition and localization-induction models correspond to externally and internally maintained condensates in Weber *et al.* [62], respectively. We clarified a crucial assumption, the differential enrichment of the kinase, phosphatase, or ATP [63] inside and outside condensates for efficient size regulation. Without this enrichment, the chemical potential of phosphorylated and unphosphorylated proteins would be almost constant in space, the net fluxes would be minimal, and size regulation would be impossible (section 5 in the supplemental information online).

The regulation of many biomolecular condensates may be more complex than the simplified models presented here. First, condensates will usually be regulated by several kinases or post-translational modifiers and they exert a combined effect on interactions within the condensate. For instance, at least two kinases, CDK2-cyclinE and VRK1, regulate the formation of Cajal bodies, but VRK1 phosphorylation of coilin at Ser184 stabilizes it against proteasomal degradation and therefore has an opposing effects on Cajal body stability [42,64]. In DNA double-strand break repair, condensate formation is regulated by both poly(ADP-ribose)ylation and phosphorylation of key proteins such as FUS [9,65,66]. Second, some processes will be regulated in a multistep fashion. For example, in signaling cascades, different types of condensate subdomains might form at each cascade step, each regulated by a different kinase and each depending on the previous one for the activation of its condensate-regulating kinase. Despite such regulatory complexity, we surmise that the regulation of condensates can often be understood by combining the two simple models.

The enrichment-inhibition model offers an explanation for the relatively low kinase specificity that is frequently observed in *in vitro* phosphorylation experiments and often deviates from the kinase specificity *in vivo* [67]. Kinases might attain most of their specificity not from their catalytic domain but from their enrichment in specific types of biocondensates. The latter is likely to be mostly determined by their disordered regions and peptide-binding modules. This hypothesis is supported by the high fraction of disorder in protein kinases and cyclins.

A crucial property of biocondensates is their ability to switch processes or biochemical reactions on or off in response to a signal comprising only a few molecules, such as a DNA double-strand break. The extremely cooperative behavior of phase transitions (even for very small condensates) explains how such weak signals can be amplified through condensate formation to recruit a multitude of factors required to react to the signal. To understand the magnitude by which condensates can accelerate reaction kinetics [68], assume that n proteins are required to form an oligomeric complex. If each component is enriched tenfold in the condensate, by mass action the oligomerization rate would be $\sim 10^n$-fold increased. Another advantage of active regulation is the thresholding behavior it produces (Figures 2C and 3C), which can suppress low-intensity noise and improve the robustness of cellular decisions.

It is becoming clear that liquid–liquid phase separation is a fundamental concept underlying most aspects of cellular regulation in eukaryotes. We hope the presented models can help to guide experiments in elucidating the functions of biocondensates and to understand their manifold roles in human diseases [66] (see Outstanding Questions).

Outstanding Questions

Which phosphatase antagonizes DYRK3 in the dissolution of membraneless organelles during mitosis and is it depleted there? Is the phosphatase PPTR-1, which antagonized MBK-2, indeed depleted in P granules?

Does the scaffolded condensate model describe enhancer and promoter condensates? What mechanism causes the observed, intermittent formation and dissolution [26]?

Neuronal granules are RNA–protein condensates serving as containers for transportation to dendrites and axons [21,22,23]. Are their assembly, disassembly, and size regulated by localization induction? What is the inducing enzyme and how is it activated and inactivated at the loading and discharge sites?

Given the involvement of the condensate-forming proteins FUS, TDP-43, and tau in neurodegenerative diseases [2,22], what are their mechanisms of condensate size control and what kinases and phosphatases regulate their condensate-forming potential?

What sequence characteristics distinguish target proteins in condensates regulated by enrichment inhibition from those in localization-inhibition-regulated ones – net charge?

Acknowledgments

We thank Matthew Grieshop for discussions and Klaus Förstemann, Michael Sattler, Axel Imhof, Melina Schuh, Eli Levy Karin, and Franco Simonetti for feedback on the manuscript. J.S. acknowledges support by grants SPP1935 and SPP2191 of the Deutsche Forschungsgemeinschaft.

Supplemental Information

Supplemental Information can be found online at https://doi.org/10.1016/j.tcb.2019.10.006.

Please cite this article in press as: Söding et al., Mechanisms for Active Regulation of Biomolecular Condensates, Trends in Cell Biology (2019), https://doi.org/10.1016/j.tcb.2019.10.006

References

1. Banani, S.F. *et al.* (2017) Biomolecular condensates: organizers of cellular biochemistry. *Nat. Rev. Mol. Cell Biol.* 18, 285–298
2. Shin, Y. and Brangwynne, C.P. (2017) Liquid phase condensation in cell physiology and disease. *Science* 357, eaaf4382
3. Wippich, F. *et al.* (2013) Dual specificity kinase DYRK3 couples stress granule condensation/dissolution to mTORC1 signaling. *Cell* 152, 791–805
4. Rai, A.K. *et al.* (2018) Kinase-controlled phase transition of membraneless organelles in mitosis. *Nature* 559, 211–216
5. Berchtold, D. *et al.* (2018) A systems-level study reveals regulators of membrane-less organelles in human cells. *Mol. Cell* 72, 1035–1049
6. Bah, A. and Forman-Kay, J.D. (2016) Modulation of intrinsically disordered protein function by post-translational modifications. *J. Biol. Chem.* 291, 6696–6705
7. Wang, J. *et al.* (2018) A molecular grammar governing the driving forces for phase separation of prion-like RNA binding proteins. *Cell* 174, 688–699
8. Dundr, M. and Misteli, T. (2010) Biogenesis of nuclear bodies. *Cold Spring Harb. Perspect. Biol.* 2, a000711
9. Altmeyer, M. *et al.* (2015) Liquid demixing of intrinsically disordered proteins is seeded by poly(ADP-ribose). *Nat. Commun.* 6, 8088
10. Tatavosian, R. *et al.* (2019) Nuclear condensates of the Polycomb protein chromobox 2 (CBX2) assemble through phase separation. *J. Biol. Chem.* 294, 1451–1463
11. Banjade, S. and Rosen, M.K. (2014) Phase transitions of multivalent proteins can promote clustering of membrane receptors. *eLife* 3, e04123
12. Case, L.B. *et al.* (2019) Regulation of transmembrane signaling by phase separation. *Ann. Rev. Biophys.* 48, 465–494
13. So, C. *et al.* (2019) A liquid-like spindle domain promotes acentrosomal spindle assembly in mammalian oocytes. *Science* 364, eaat9557
14. Jiang, H. *et al.* (2015) Phase transition of spindle-associated protein regulates spindle apparatus assembly. *Cell* 163, 108–122
15. Ukmar-Godec, T. *et al.* (2019) Lysine/RNA-interactions drive and regulate biomolecular condensation. *Nat. Commun.* 10, 2909
16. Weirich, K.L. *et al.* (2017) Liquid behavior of cross-linked actin bundles. *Proc. Natl Acad. Sci. U. S. A.* 114, 2131–2136
17. Bergeron-Sandoval, L.-P. *et al.* (2018) Endocytosis caused by liquid–liquid phase separation of proteins. *bioRxiv.* .Published online December 4, 2018. https://doi.org/10.1101/145664.
18. Miao, Y. *et al.* (2018) Phospho-regulation of intrinsically disordered proteins for actin assembly and endocytosis. *FEBS J.* 285, 2762–2784
19. Wu, X. *et al.* (2019) RIM and RIM-BP form presynaptic active-zone-like condensates via phase separation. *Mol. Cell* 73, 971–984
20. Zeng, M. *et al.* (2018) Reconstituted postsynaptic density as a molecular platform for understanding synapse formation and plasticity. *Cell* 174, 1172–1187
21. Liao, Y.-C. *et al.* (2019) RNA granules hitchhike on lysosomes for long-distance transport, using annexin A11 as a molecular tether. *Cell* 179, 147–164
22. Alami, N.H. *et al.* (2014) Axonal transport of TDP-43 mRNA granules is impaired by ALS-causing mutations. *Neuron* 81, 536–543
23. Formicola, N. *et al.* (2019) Neuronal RNP granules: dynamic sensors of localized signals. *Traffic* 20, 639–649
24. Cho, W.-K. *et al.* (2018) Mediator and RNA polymerase II clusters associate in transcription-dependent condensates. *Science* 361, 412–415
25. Sabari, B.R. *et al.* (2018) Coactivator condensation at super-enhancers links phase separation and gene control. *Science* 361, eaar3958
26. Chong, S. *et al.* (2018) Imaging dynamic and selective low-complexity domain interactions that control gene transcription. *Science* 361, eaar2555
27. Boehning, M. *et al.* (2018) RNA polymerase II clustering through carboxy-terminal domain phase separation. *Nat. Struct. Mol. Biol.* 25, 833
28. Hyman, A.A. *et al.* (2014) Liquid–liquid phase separation in biology. *Annu. Rev. Cell Dev. Biol.* 30, 39–58
29. Weidtkamp-Peters, S. *et al.* (2008) Dynamics of component exchange at PML nuclear bodies. *J. Cell Sci.* 121, 2731–2743
30. Qamar, S. *et al.* (2018) FUS phase separation is modulated by a molecular chaperone and methylation of arginine cation-π interactions. *Cell* 173, 720–734
31. Nott, T.J. *et al.* (2015) Phase transition of a disordered nuage protein generates environmentally responsive membraneless organelles. *Mol. Cell* 57, 936–947
32. Gibson, B.A. *et al.* (2019) Organization and regulation of chromatin by liquid–liquid phase separation. *bioRxiv.* Published online January 18, 2019. https://doi.org/10.1101/523662.
33. Danieli, A. and Martens, S. (2018) P62-mediated phase separation at the intersection of the ubiquitin-proteasome system and autophagy. *J. Cell Sci.* 131, jcs214304
34. Drino, A. and Schaefer, M.R. (2018) RNAs, phase separation, and membrane-less organelles: are post-transcriptional modifications modulating organelle dynamics? *Bioessays* 40, 1800085
35. Ries, R.J. *et al.* (2019) M^6A enhances the phase separation potential of mRNA. *Nature* 571, 424–428
36. Hondele, M. *et al.* (2019) DEAD-box ATPases are global regulators of phase-separated organelles. *Nature* 573, 144–148
37. Wang, J.T. *et al.* (2014) Regulation of RNA granule dynamics by phosphorylation of serine-rich, intrinsically disordered proteins in *C. elegans*. *eLife* 3, e04591
38. Wurtz, J.D. and Lee, C.F. (2018) Stress granule formation via ATP depletion-triggered phase separation. *New J. Phys.* 20, 045008
39. Spector, D.L. and Lamond, A.I. (2011) Nuclear speckles. *CSH Perspect. Biol.* 3, a000646
40. Kwon, I. *et al.* (2014) Poly-dipeptides encoded by the *C9orf72* repeats bind nucleoli, impede RNA biogenesis, and kill cells. *Science* 345, 1139–1145
41. Colwill, K. *et al.* (1996) The Clk/Sty protein kinase phosphorylates SR splicing factors and regulates their intranuclear distribution. *EMBO J.* 15, 265–275
42. Liu, J. *et al.* (2000) Cell cycle-dependent localization of the CDK2–cyclin E complex in Cajal (coiled) bodies. *J. Cell Sci.* 113, 1543–1552
43. Milovanovic, D. *et al.* (2018) A liquid phase of synapsin and lipid vesicles. *Science* 361, 604–607
44. Chamma, I. *et al.* (2016) Mapping the dynamics and nanoscale organization of synaptic adhesion proteins using monomeric streptavidin. *Nat. Commun.* 7, 10773
45. Thievessen, I. *et al.* (2013) Vinculin–actin interaction couples actin retrograde flow to focal adhesions, but is dispensable for focal adhesion growth. *J. Cell Biol.* 202, 163–177

46. Rogacki, M.K. *et al.* (2018) Dynamic lateral organization of opioid receptors (kappa, mu_{wt} and mu_{N40D}) in the plasma membrane at the nanoscale level. *Traffic* 19, 690–709
47. Langelier, M.-F. *et al.* (2012) Structural basis for DNA damage-dependent poly(ADP-ribosyl)ation by human PARP-1. *Science* 336, 728–732
48. Mortusewicz, O. *et al.* (2011) PARG is recruited to DNA damage sites through poly(ADP-ribose)- and PCNA-dependent mechanisms. *Nucleic Acids Res* 39, 5045–5056
49. Su, X. *et al.* (2016) Phase separation of signaling molecules promotes T cell receptor signal transduction. *Science* 352, 595–599
50. Conduit, P.T. *et al.* (2015) Centrosome function and assembly in animal cells. *Nat. Rev. Mol. Cell Biol.* 16, 611–624
51. Conduit, P.T. *et al.* (2010) Centrioles regulate centrosome size by controlling the rate of Cnn incorporation into the PCM. *Curr. Biol.* 20, 2178–2186
52. Shrinivas, K. *et al.* (2019) Enhancer features that drive formation of transcriptional condensates. *Mol. Cell* 75, 549–561.e7
53. Nair, S.J. *et al.* (2019) Phase separation of ligand-activated enhancers licenses cooperative chromosomal enhancer assembly. *Nat. Struct. Mol. Biol.* 26, 193–203
54. Fox, A.H. *et al.* (2018) Paraspeckles: where long noncoding RNA meets phase separation. *Trends Biochem. Sci.* 43, 124–135
55. Decker, M. *et al.* (2011) Limiting amounts of centrosome material set centrosome size in *C. elegans* embryos. *Curr. Biol.* 21, 1259–1267
56. Zwicker, D. *et al.* (2014) Centrosomes are autocatalytic droplets of pericentriolar material organized by centrioles. *Proc. Natl Acad. Sci. U. S. A.* 111, E2636–E2645
57. Du, M. and Chen, Z.J. (2018) DNA-induced liquid phase condensation of cGAS activates innate immune signaling. *Science* 361, 704–709
58. Narayanan, A. *et al.* (2019) A first order phase transition mechanism underlies protein aggregation in mammalian cells. *eLife* 8, e39695
59. Feric, M. and Brangwynne, C.P. (2013) A nuclear F-actin scaffold stabilizes ribonucleoprotein droplets against gravity in large cells. *Nat. Cell Biol.* 15, 1253
60. Zwicker, D. *et al.* (2015) Suppression of Ostwald ripening in active emulsions. *Phys. Rev. E* 92, 012317
61. Wurtz, J.D. and Lee, C.F. (2018) Chemical-reaction-controlled phase separated drops: formation, size selection, and coarsening. *Phys. Rev. Lett.* 120, 078102
62. Weber, C.A. *et al.* (2019) Physics of active emulsions. *Rep. Prog. Phys.* 82, 064601
63. Patel, A. *et al.* (2017) ATP as a biological hydrotrope. *Science* 356, 753–756
64. Cantarero, L. *et al.* (2015) VRK1 regulates Cajal body dynamics and protects coilin from proteasomal degradation in cell cycle. *Sci. Rep.* 5, 10543
65. Monahan, Z. *et al.* (2017) Phosphorylation of the FUS low-complexity domain disrupts phase separation, aggregation, and toxicity. *EMBO J.* 36, 2951–2967
66. Wang, Z. and Zhang, H. (2019) Phase separation, transition, and autophagic degradation of proteins in development and pathogenesis. *Trends Cell Biol.* 29, 417–427
67. Miller, C.J. and Turk, B.E. (2018) Homing in: mechanisms of substrate targeting by protein kinases. *Trends Biochem. Sci.* 43, 380–394
68. Stroberg, W. and Schnell, S. (2018) Do cellular condensates accelerate biochemical reactions? Lessons from microdroplet chemistry. *Biophys. J.* 115, 3–8
69. Bracha, D. *et al.* (2018) Mapping local and global liquid phase behavior in living cells using photo-oligomerizable seeds. *Cell* 175, 1467–1480
70. Alberti, S. *et al.* (2019) Considerations and challenges in studying liquid–liquid phase separation and biomolecular condensates. *Cell* 176, 419–434
71. Ramachandran, V. *et al.* (2011) The cAMP-dependent protein kinase signaling pathway is a key regulator of P body foci formation. *Mol. Cell.* 43, 973–981

Supplemental Information

Mechanisms for active regulation of biomolecular condensates

Johannes Söding,[1,*] David Zwicker,[2] Salma Sohrabi-Jahromi,[1] Marc Boehning,[3] Jan Kirschbaum[2]

[1] Quantitative Biology & Bioinformatics and [3] Department of Molecular Biology,
Max-Planck Institute for Biophysical Chemistry, Am Fassberg 11, 37077 Göttingen, Germany.
[2] Max-Planck Institute for Dynamics & Self-Organization, Am Fassberg 17, 37077 Göttingen, Germany.
[*] Correspondence: soeding@mpibpc.mpg.de (J. Söding)

1. Condensate droplet growth and shrinkage in a passive, phase-separating system

1.1 Protein concentration $c_R(R)$ just outside a condensate of radius R

We derive here the formula for the protein concentration just outside a condensate of radius R (Figure S1A),

$$c_R(R) = c_{\text{out}} \left(1 + \frac{l_c}{R}\right) , \tag{1}$$

where c_{out} is the concentration outside a condensate droplet of infinite radius $R \to \infty$ and l_c is the capillary length, a measure of the strength of interaction between the proteins (defined in eq. (7)).

We call the protein concentration inside the condensate c_{in}. Imagine to transfer from just outside to the inside of the condensate a single protein, together with just the right amount of solvent such that this tiny volume dV has the same concentration as the inside of the droplet. That means $1 = dV\, c_{\text{in}}$, or $dV = c_{\text{in}}^{-1}$. The radius of the condensate will increase from R to $R + dR$. dR can be obtained by solving the equation for the conservation of volume $(4\pi/3)(R + dR)^3 = (4\pi/3)R^3 + dV$, yielding

$$dR = dV/(4\pi R^2) . \tag{2}$$

The change in free energy for the transfer must be zero at equilibrium between the two phases. The change of free energy is the change in interaction energy ΔE plus the effect of change in entropy $-T\Delta S$ (with T the absolute temperature),

$$\Delta F = \Delta E - T\Delta S = 0 \tag{3}$$

We define $-\varepsilon$ as the change in interaction energy of the protein when transferred from the outside of an infinitely extended phase ($R \to \infty$) to the inside. The change is slightly lower for a finite-sized condensate of radius R, due to surface tension:

$$\begin{aligned} \Delta E &= -\varepsilon + 4\pi(R + dR)^2\gamma - 4\pi R^2\gamma \\ &= -\varepsilon + 8\pi\gamma\, R dR + \cancel{\text{const.} \times (dR)^2} \\ &= -\varepsilon + \frac{2dV\gamma}{R} . \end{aligned} \tag{4}$$

where the term $2dV\gamma/R = 2\gamma/(c_{\text{in}}\, R)$ describes the work done against the surface tension γ of the condensate. The entropy change is

$$\Delta S = k_B \log c_R(R) - k_B \log c_{\text{in}} , \tag{5}$$

with Boltzmann's constant k_B. Putting everything together, we obtain

$$k_B T \log \frac{c_R(R)}{c_{in}} = -\varepsilon + \frac{2\gamma}{c_{in} R}\,. \tag{6}$$

Defining the capillary length,

$$l_c = \frac{2\,\gamma}{k_B T\, c_{in}}\,, \tag{7}$$

we get

$$c_R(R) = c_{in}\, e^{-\frac{\varepsilon}{k_B T}}\, e^{l_c/R}\,. \tag{8}$$

By setting R to ∞, we obtain $c_{out} = c_\infty(\infty) = c_{in}\, e^{-\frac{\varepsilon}{k_B T}}$ and therefore

$$c_R(R) = c_{out}\, e^{l_c/R} \approx c_{out}\left(1 + \frac{l_c}{R}\right)\,. \tag{9}$$

The approximation is accurate for $l_c/R \ll 1$. This finite-R correction term is proportional to $2\gamma/R$, called Laplace pressure in physics.

1.2 Concentration $c_R(r)$ around a condensate of radius R and net flux out of condensate

We imagine that only a single condensate of radius R floats in the dilute phase of infinite extension, and the protein concentration at infinite distance r from the condensate center is c_∞. For symmetry reasons, the protein concentration will be the same everywhere on a spherical shell of radius r around the condensate, so we can write it as a $c_R(r)$.

From statistical physics we know that a concentration gradient ∇p causes a net diffusive flux density j in the opposite direction of the gradient, measured in particles per second per area through which the particles diffuse: $\mathbf{j} = -D\nabla p$. The proportionality constant is the diffusion coefficient D. Applied to our system, the flux density through a spherical shell of radius r around the condensate is

$$j(r) = -D\frac{\partial}{\partial r} c_R(r)\,. \tag{10}$$

The total flux integrated over the entire shell surface $4\pi r^2$ is therefore $-4\pi D r^2 \frac{\partial c_R(r)}{\partial r}$. At equilibrium concentrations, (and, in the active systems discussed in Figures 2 and 3, for low rates of (de-)phosphorylation) the flux through each sphere of radius $r > R$ must be constant, since no proteins can be created or lost between shells:

$$\text{const.} = -4\pi D r^2 \frac{\partial}{\partial r} c_R(r)\,. \tag{11}$$

This differential equation is solved by $c_R(r) = \alpha + \beta/r$. To obtain α and β, we use the boundary conditions at $r = R$ and $r = \infty$,

$$c_R(R) = \alpha + \beta/R = c_{out}\left(1 + \frac{l_c}{R}\right) \tag{12}$$

$$c_R(\infty) = \alpha = c_\infty\,. \tag{13}$$

From this it follows that $\beta = [c_R(R) - c_R(\infty)]R$ and

$$c_R(r) = c_\infty + (c_\infty - c_{out})\left(-1 + \frac{R_{crit}}{R}\right)\frac{R}{r} \tag{14}$$

with

$$R_{crit} = \frac{c_{out}}{c_\infty - c_{out}} l_c\,. \tag{15}$$

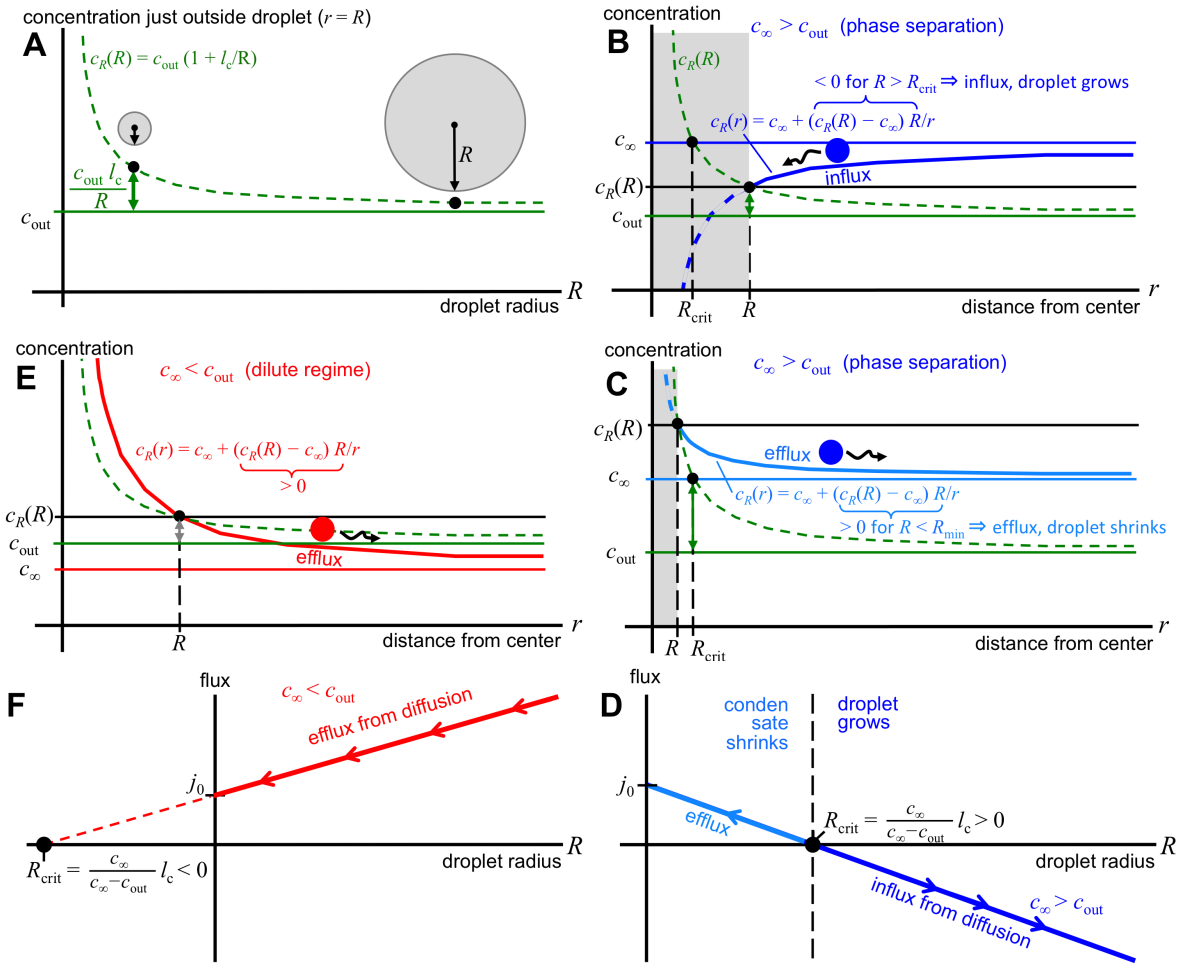

Figure S1: **Concentration and flux around liquid droplet condensates in a passive system.** (A) The protein concentration just outside a condensate of radius R is higher by $c_{out}l_c/R$ than the concentration c_{out} outside an infinitely extended phase ($R \to \infty$). (B) Protein concentration around a condensate of radius R if the concentration c_∞ at distance $r \to \infty$ is larger than c_{out} and condensates above the critical radius, $R > R_{crit}$. (C) Protein concentration for the case $c_\infty > c_{out}$ and condensates with $R < R_{crit}$. (D) Net diffusive flux out of condensates of size R for $c_\infty > c_{out}$. (E) Protein concentration if $c_\infty < c_{out}$. (F) Net diffusive flux out of condensates of size R for $c_\infty < c_{out}$.

The total flux of proteins leaving the condensate is

$$\text{flux} = 4\pi D R^2 \left.\frac{\partial c_R(r)}{\partial r}\right|_{r=R} \tag{16}$$

$$= -4\pi D(c_\infty - c_{out})(R - R_{crit})\,. \tag{17}$$

This result is plotted in Figure S1D for the case $c_\infty > c_{out}$. In that case, for condensates above the critical radius, $R > R_{crit}$, the concentration decreases towards the condensate, and the net flux flows towards the condensate (Figure S1B), making the condensate grow. For condensates below the critical radius, $R < R_{crit}$, the concentration increases towards the condensate and the net flux flows away from the condensate (Figure S1C), making the condensate shrink.

For the case $c_\infty < c_{out}$ (Figures S1E,F), the concentration increases towards the condensates for any radius, and the condensate flux will be directed outwards, shrinking the condensate. The critical radius for this case is negative and the flux depends on the radius as shown in Figure S1F.

1.3. Time scale of droplet coarsening

The coarsening of droplets is due to a diffusive protein flux from small to large droplets, which is caused by small droplets having a larger equilibrium concentration $c_R(R)$ right outside their interface than large droplets (eq. (1)). To estimate the characteristic time scale τ, we note that the rate of change of the volume of a droplet of radius R is equal to $1/c_{\rm in}$ times the total net flux into the droplet in equation (17), measured in number of proteins per second:

$$\begin{aligned}\frac{d}{dt}\left(\frac{4\pi}{3}R^3\right) &= \frac{1}{c_{\rm in}}4\pi D(c_\infty - c_{\rm out})(R - R_{\rm crit}) \\ \frac{dR}{dt} &= \frac{D}{R^2}\frac{c_\infty - c_{\rm out}}{c_{\rm in}}(R - R_{\rm crit})\,. \end{aligned} \tag{18}$$

Using equation (15) and noting that $R_{\rm crit}$ changes much more slowly than R,

$$\begin{aligned}\frac{d}{dt}(R - R_{\rm crit}) \approx \frac{dR}{dt} &= \frac{D\,l_{\rm c}}{R^2 R_{\rm crit}}\frac{c_{\rm out}}{c_{\rm in}}(R - R_{\rm crit}) \\ \frac{d}{dt}(R - R_{\rm crit}) &\approx \frac{1}{\tau}(R - R_{\rm crit}) \end{aligned} \tag{19}$$

where

$$\tau(R) = \frac{R^2 R_{\rm crit}}{D\,l_{\rm c}}\frac{c_{\rm in}}{c_{\rm out}} \tag{20}$$

gives the approximate time for $R - R_{\rm crit}$ to change by a factor $e = 2.718$. Consequently, τ is the time scale for coarsening.

To estimate τ, we find the approximate protein concentration inside the condensate $c_{\rm in}$ by assuming a 1:1 ratio of protein to water and a protein density similar to water, 1 kg/l. Using a protein molecular weight of 30 kDa, we get $c_{\rm in} \approx 0.5 \times 1{\rm kg/l}/30{\rm kDa} = 10^{22}/{\rm l} = 17\,{\rm mM}$. With this value, assuming a typical surface tension for the condensate of $\gamma = 1$ pN/μm, and using equation (7), the capillary length is $l_{\rm c} = 2\gamma/(k_{\rm B}Tc_{\rm in}) \approx 0.5$ Å. We further conservatively estimate the protein enrichment in the condensate to be $c_{\rm in}/c_{\rm out} \approx 100$. Using a typical diffusivity of $D = 10\ \mu{\rm m}^2/{\rm s}$ [1], we estimate τ for droplets of radius $R \approx R_{\rm crit} \approx 100\,{\rm nm}$ as $\tau_{100{\rm nm}} \approx 3$ minutes. For a radius of 1 μm, this becomes 1000 times larger, or $\tau_{1\mu{\rm m}} \approx 2$ days.

2. Threshold radius $R_{\rm thr}$ and condensate radius $R(k)$ for the enrichment-inhibition model

The model assumes that length scale of reaction-diffusion is long in comparison to the droplet radius. If this assumption was violated, unphosphorylated proteins would not replenished fast enough and condensates could not be stable.

For the enrichment-inhibition model, we can determine the threshold radius $R_{\rm thr}$ (Fig. 2B) by solving R under the constraints that

$$\frac{\partial}{\partial R}{\rm flux}(R_{\rm thr}) = 0 \tag{21}$$

$${\rm flux}(R) = 0\,. \tag{22}$$

We insert the total flux

$${\rm flux}(R) = -4\pi D(c_\infty - c_{\rm out})(R - R_{\rm crit}) + \frac{4\pi}{3}R^3 c_{\rm in}k \tag{23}$$

and obtain

$$-4\pi D(c_\infty - c_{\rm out}) + 4\pi R^2 c_{\rm in}k = 0 \tag{24}$$

$$-\cancel{4\pi D(c_\infty - c_{\rm out})}(R - R_{\rm crit}) - \frac{1}{3}R\,\cancel{4\pi D(c_\infty - c_{\rm out})} = 0 \tag{25}$$

and hence

$$R_{\rm thr} = \frac{3}{2} R_{\rm crit} = \frac{3}{2} \frac{c_\infty}{c_\infty - c_{\rm out}} l_{\rm c} \,. \tag{26}$$

To find the condensate radius $R(k)$ for a given phosphorylation rate per volume, k, with

$$k \propto c_{\rm kinase,in}\, c_{\rm ATP,in} \,, \tag{27}$$

one can simply solve the cubic equation $\mathrm{flux}(R) = 0$, which has an analytical solution (Cardano formula).

3. Condensate radius $R(Q)$ for the localization-induction model

The radius $R(Q)$ follows from the zero total flux condition

$$\mathrm{flux}(R) = -4\pi D(c_\infty - c_{\rm out})(R - R_{\rm crit}) - Q = 0, \tag{28}$$

where Q is the total amount of phosphorylated proteins per time supplied to the condensate by the localized kinase. This yields, for $c_\infty < c_{\rm out}$

$$R(Q) = \frac{Q}{4\pi D(c_{\rm out} - c_\infty)} + R_{\rm crit} = \frac{c_\infty}{c_{\rm out} - c_\infty} \left(\frac{Q}{4\pi D c_\infty} - l_{\rm c} \right) . \tag{29}$$

4. Size regulation of transmembrane receptor clusters

Many transmembrane receptors organize into dense, supramolecular clusters of a certain preferred size upon binding to extracellular ligands [2, 3, 4, 5]. A fixed cluster size can be advantageous: Clusters need to be large enough for the kinase activity of the entire cluster to surpass the threshold rate $k_{\rm thr}$ for forming a localized liquid droplet at the membrane (Figure 3C). On the other hand, the uncontrolled size of receptor clusters would lead to an uncontrolled size of the localized droplets inside. Also, outsized clusters would deplete receptors and suppress signal transduction elsewhere.

Analogous to three dimensions, phase separation can occur also in two dimensions above a certain saturation surface density [6, 2], with the formation of clusters of high density surrounded by low-density regions. If ligand-bound receptors interacted while unbound ones did not, or more weakly, increasing the ligand concentration and thus the fraction of ligand-bound receptors would increase the surface density of ligand-bound, interacting receptors. When that density is pushed above the 2D saturation threshold, clusters would form. The mechanism would nicely explains the sharp onset of cluster formation upon a small change of ligand density. However, analogous to the 3D case, coarsening would lead to the growth of large clusters and shrinkage of small ones, not to clusters of fixed sizes.

Biophysical models can in principle explain the formation of clusters of fixed size by an interplay of short-range attraction between receptors and long-range repulsion [2, 7] (just like the attractive, short-range strong nuclear force and the repulsive, long-range electrostatic force between protons in atomic nuclei explains the "valley of stability"). However, this model requires weak electrostatic screening [2, 7], more precisely, the Debye length for the exponential decay of electric fields around charges must be at least on the order of the cluster size, whereas in fact in cells the Debye length is probably below a nanometer [8].

The following two-dimensional version of the localization-induction model might explain how the cluster sizes can be regulated. Transmembrane receptors can exist in three states, unbound, bound, and phosphorylated. Ligand-bound receptors can cross-phosphorylate other receptors, unbound ones cannot. Active receptors get inactivated by dephosphorylation by a phosphatase with a certain rate. A stable cluster size should be achievable under the assumption that phosphorylated receptors bind

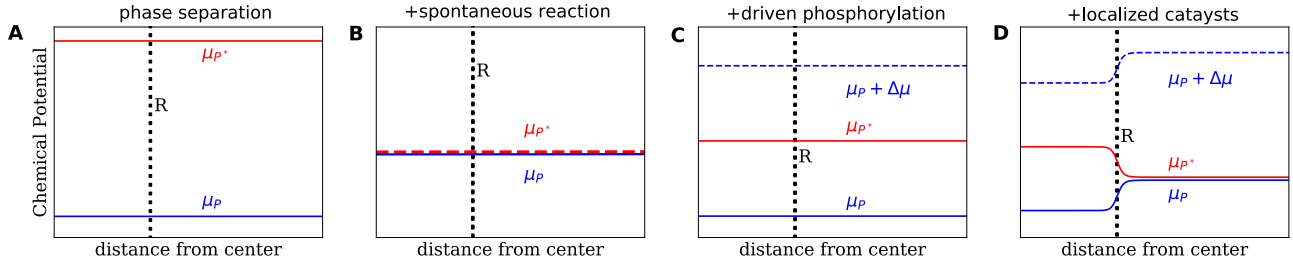

Figure S2: Schematic of the chemical potential of the unphosphorylated protein P (blue lines) and the phosphorylated protein P^* (red lines) for different reaction schemes. **A** In the case of passive phase separation, the chemical potentials equilibrate independently. Consequently, gradients in chemical potential are absent and diffusive fluxes do not exist. **B** Adding spontaneous (de-)phosphorylation ($P \rightleftharpoons P^*$) implies the chemical equilibrium $\mu_P = \mu_{P^*}$. **C** Additionally driving the phosphorylation by ATP ($P + \mathrm{ATP} \rightleftharpoons P^* + \mathrm{ADP}$) keeps the system away from equilibrium if ATP levels are maintained. However, if the reactions proceed equally in both phases phosphorylation and dephosphorylation can be balanced locally. Consequently, spatial fluxes do not exist although the energy $\Delta\mu = \mu_{\mathrm{ATP}} - \mu_{\mathrm{ADP}}$ supplied by ATP is consumed. **D** Biasing the reactions, e.g. by localizing kinases and phosphatases in different phases, induces spatial fluxes and allows for size control.

to each other with higher affinity than unphosphorylated ones. Importantly, this assumption, which requires phosphorylation as an active, driven process, makes the ligand off-rate independent of whether the receptor is part of a cluster or not.

When a receptor gets dephosphorylated, the receptor can be lost from the cluster. If the mean net distance that unphosphorylated receptors travel by diffusion until it gets rephosphorylated is large in comparison to the cluster size, most receptor dephosphorylations will result in the loss or the receptor from the cluster, yielding a loss rate proportional to the number of receptors in the cluster times the phosphorylation rate, hence proportional to its radius squared, R^2. If the mean net distance travelled is much smaller than the droplet radius R, only a fraction of receptors dephosphorylated near to the edge of the cluster will get lost from the cluster. In this case, the loss rate is proportional the circumference of the cluster, $2\pi R$.

The loss is compensated by the influx of inactive receptors, which will be phosphorylated through contact with ligand-bound receptors in the cluster. The influx can be shown to roughly be proportional to $(\log d/R)^{-1}$, where $d = (\pi\rho)^{-1/2}$ is the root mean squared distance between clusters and ρ is the number of clusters of size R per cell surface area. The balance between the influx dropping with increasing R and the loss growing with R or R^2 can then yield in a stable cluster size R.

5. Enrichment of kinase, phosphatase or ATP is necessary for size stabilization

In simple systems without chemical reactions, biochemical condensates are regions enriched in droplet material that are in equilibrium with the surrounding solvent such that the chemical potentials are constant in space ($\mu_i = \text{const.}$); see Fig. S2A. Consequently, no spatial fluxes (which would be driven by gradients in chemical potential) exist. Because of surface tension, large droplets are energetically favorable, so that the equilibrium state is a single droplet whose size is determined by the total amount of phase separating material in the system.

If the droplet material can spontaneously transition between two states (e.g., between a phosphorylated state P^* and a dephosphorylated state P) the associated chemical potentials will equilibrate at every point in space ($\mu_{P^*} = \mu_P$). In this case the reaction will change the relative amount of P and P^* compared to the passive case, but after this chemical equilibration, the system is passive and no fluxes exist; see Fig. S2B.

Chemical fluxes can be sustained by input of external energy, e.g. by using ATP to phosphorylate P continuously. Since the metabolism of the cell maintains the chemical potentials of ATP, ADP, and phosphate constant, the conversion $P \rightleftharpoons P^*$ with and without ATP cannot equilibrate at the same time. However, if these reactions proceed at the same rate everywhere, the phosphorylation driven by ATP will eventually be balanced by the dephosphorylation not involving ATP; see Fig. S2C. Consequently, although ATP is used continuously, there are still no spatial fluxes and the condensates behave qualitatively similar to the passive ones.

Kinases and phosphatases act as catalysts for the (de-)phosphorylation reaction, changing the reaction rates but not the equilibrium states. However, if the catalysts co-localize with the proteins, the reaction is biased towards different states inside and outside the condensate. This local bias leads to a chemical potential difference between the condensate and the surrounding, which drives spatial fluxes and can lead to a suppression of coarsening; see Fig. S2D. A strong segregation of kinases and phosphatases in different phases leads to strong spatial fluxes and thereby to a high conversion efficiency between the two species.

References

1 Tomoki Matsuda, Atsushi Miyawaki, and Takeharu Nagai. Direct measurement of protein dynamics inside cells using a rationally designed photoconvertible protein. *Nature Methods*, 5(4):339, 2008.

2 Lindsay B Case, Jonathon A Ditlev, and Michael K Rosen. Regulation of transmembrane signaling by phase separation. *Ann. Rev. Biophysics*, 48:465–494, 2019.

3 Ingrid Chamma, Mathieu Letellier, Corey Butler, Béatrice Tessier, Kok-Hong Lim, Isabel Gauthereau, Daniel Choquet, Jean-Baptiste Sibarita, Sheldon Park, Matthieu Sainlos, and Olivier Thoumine. Mapping the dynamics and nanoscale organization of synaptic adhesion proteins using monomeric streptavidin. *Nature Commun.*, 7:10773, 2016.

4 Ingo Thievessen, Peter M Thompson, Sylvain Berlemont, Karen M Plevock, Sergey V Plotnikov, Alice Zemljic-Harpf, Robert S Ross, Michael W Davidson, Gaudenz Danuser, Sharon L Campbell, et al. Vinculin–actin interaction couples actin retrograde flow to focal adhesions, but is dispensable for focal adhesion growth. *J. Cell Biol.*, 202(1):163–177, 2013.

5 Maciej K Rogacki, Ottavia Golfetto, Steven J Tobin, Tianyi Li, Sunetra Biswas, Raphael Jorand, Huiying Zhang, Vlad Radoi, Yu Ming, Per Svenningsson, Daniel Ganjali, Devin L. Wakefield, Athanasios Sideris, Alexander R Small, Lars Terenius, Tijana Jovanović-Talisman, and Vladana Vukojević. Dynamic lateral organization of opioid receptors (kappa, $\mathrm{mu_{wt}}$ and $\mathrm{mu_{N40D}}$) in the plasma membrane at the nanoscale level. *Traffic*, 19(9):690–709, 2018.

6 Sudeep Banjade and Michael K Rosen. Phase transitions of multivalent proteins can promote clustering of membrane receptors. *Elife*, 3:e04123, 2014.

7 Anna Stradner, Helen Sedgwick, Frédéric Cardinaux, Wilson CK Poon, Stefan U Egelhaaf, and Peter Schurtenberger. Equilibrium cluster formation in concentrated protein solutions and colloids. *Nature*, 432(7016):492, 2004.

8 Jan J Spitzer and Bert Poolman. Electrochemical structure of the crowded cytoplasm. *Trends Biochem. Sci.*, 30(10):536–541, 2005.